Proceedings of the Korean Nuclear Society Spring Meeting
Cheju, Korea, May 2001

High Energy Nuclear Data Evaluations for Neutron-, Proton-, and Photon-Induced Reactions at KAERI

Young-Ouk Lee, Jonghwa Chang, Doohwan Kim, Jeong-Yeon Lee
Korea Atomic Energy Research Institute
P.O. Box 105 Yusong, Taejon 305-600, Korea

Yinlu Han
China Institute of Atomic Energy, China

Efrem Sh. Sukhovitski
Radiation Physics and Chemistry Problems Institute
220109, Minsk-Sosny, Belarus

The Korea Atomic Energy Research Institute (KAERI) is building high energy neutron-, proton-, and photon-induced nuclear data libraries for energies up to hundreds MeV in response to nuclear data needs from various R&Ds and applications. The librares provide nuclear data needed for the accelerator-driven transmutation of nuclear waste and radiation transport simulations of cancer radiotherapy. The neutron library currently has 10 isotopes such as C-12, N-14, O-16, Al-27, Si-28, Ca-40, Fe-56, Ni-58, Zr-90, Sn-120, and Pb-208 for energies from 20 up to 400 MeV. The proton nuclear data were evaluated in a consistent manner with the neutron case, using the same nuclear model parameters. In addition to the same isotopes included in the neutron library, the proton library has 70 extra isotopes of 24 elements ranging from nitrogen to lead up to 150 MeV for which the evaluations are focused on the medical and activation analyses applications. The photonuclear data library has been built along with international collaboration by participating in the IAEA's Coordinated Research Project (CRP) which ended last year. Currently the KAERI photonuclear library includes 143 isotopes of 39 elements.

I. Introduction

Nuclear data for conventional fission reactors and fusion devices mainly consist of neutron-induced cross sections in energy below 20 MeV. However, recent new applications, such as radiation transport simulations of cancer radiotherapy and the accelerator-driven transmutation of nuclear wastes require evaluated nuclear data on neutron-, proton, and photon-induced reaction above a few MeV up to a few hundreds of MeV.

The Korea Atomic Energy Research Institute (KAERI) is building neutron-, proton-, and photon-induced nuclear data libraries for energies up to hundreds MeV in response to nuclear data needs from various R&Ds and applications [1–4]. The library provides nuclear data needed for the accelerator-driven transmutation of nuclear waste and radiation transport simulations of cancer radiotherapy [5–7]. The neutron library currently has 10 isotopes such as C-12, N-14, O-16, Al-27, Si-28, Ca-40, Fe-56, Ni-58, Zr-90, Sn-120, and Pb-208 for energies from 20 up to 400 MeV. The proton nuclear data were evaluated in a consistent manner with the neutron case, using the same nuclear model parameters. In addition to the same isotopes for the neutron case, the proton library has 70 extra isotopes of 24 elements ranging from nitrogen to lead up to 150 MeV for which the evaluations are focused on the medical and activation analyses applications. The photonuclear data library has been built along with international collaboration by participating in the IAEA's Coordinated Research Project(CRP). As a final product, 143 isotopes of 39 elements are included in the KAERI photonuclear data library [8–10].

Section 2 describes an overview of evaluation methods and theoretical models applied in this work. Section 3 provides some comparisons of evaluated cross sections with experimental data, and Section 4 summarizes the KAERI high energy libraries.

II. Evaluation Methods and Models

A typical procedure to produce the evaluated cross sections is as follows:

- Survey, analyses, and selection of reference measurements
- Applying appropriate theoretical models according to the reaction characteristics
- Selection or adjustment of the recommended model parameters to better produce the reference measurements
- Generation of the cross sections in the ENDF-6 format

Details of the procedure are described below.

1. Reference Measurements

The role of experimental data for the nuclear data evaluation is important; it guides modeling of nuclear reactions, but also validate the models and parameters. From this view point, it is desirable that the reference experimental data span over a certain number of nuclei, reactions and incident energies. For the reference data of neutron, proton, and photon induced reactions up to a few hundreds MeV region, the EXFOR [11] database was extensively surveyed and analyzed to selected reference measurements.

2. Optical Model

The optical model provides the basis for theoretical evaluations of nuclear cross sections that are used in providing nuclear data for applications. In addition to offering a convenient means for calculations of reaction, shape elastic, and (neutron) total cross sections, optical model potentials are widely used in quantum-mechanical preequilibrium and direct-reaction theory calculation. But the most important role of optical model analysis is to supply particle transmission coefficients for Hauser-Feshbach statistical theory analyses used in nuclear data evaluations.

In this work, the energy dependencies of potential depths are expressed in the following way, which is similar to that proposed by Delaroche [12]:

$$\begin{aligned} V_r(E) &= V_0 e^{-\lambda_{vr}(E-E_f)} + V_1 + V_2 E \\ W_v(E) &= W_{v0} \frac{(E-E_f)^4}{(E-E_f)^4 + W_{v1}^4} \\ W_d(E) &= W_{d0} e^{-\lambda_{wd}(E-E_f)} \frac{(E-E_f)^4}{(E-E_f)^4 + W_{d1}^4}, \\ r_i(E) &= r_{i0} + r_{i1} E \\ a_i(E) &= a_{i0} + a_{i1} E \end{aligned} \tag{1}$$

where the Fermi energy E_f for neutrons and protons is given by

$$\begin{aligned} \text{neutron} \quad & E_f(Z,A) = -\frac{1}{2}[S_n(Z,A) + S_n(Z,A+1)] \\ \text{proton} \quad & E_f(Z,A) = -\frac{1}{2}[S_p(Z,A) + S_p(Z+1,A+1)] \end{aligned} \tag{2}$$

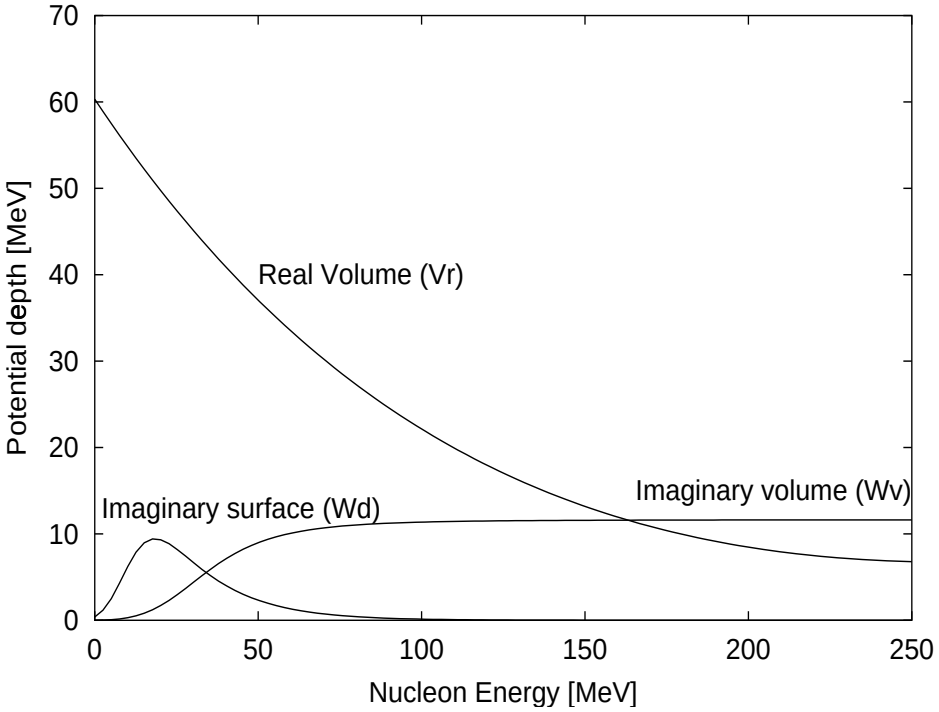

Figure 1: The volume potential depths of real volume, imaginary volume and imaginary surface as a function of neutron and proton energy

The geometry factor of W_v is assumed to be the same as that of V_r as

$$\begin{aligned} r_v(E) &= r_{wv}(E) \neq r_{wd}(E) \\ a_v(E) &= a_{wv}(E) \neq a_{wd}(E) \end{aligned} \tag{3}$$

Figure 1 presents the general shapes of the potential depths of real volume (V_r), volume absorptive (W_v) and surface absorptive (W_d) adopted in this work to incorporate effects of the dispersion relationship. The best sets of OMP were determined by adjusting the above 17 adjustable coefficients defined in eq. (1) and (3) with the use of ECISPLOT [13], an interactive optical parameter searcher with the simulated annealing algorithm, developed by one of the authors. This is an X-Window based software system incorporated into the nuclear reaction code ECIS-96 [14]. In ECISPLOT, the potential parameters are adjusted interactively based on an eye-guide, then the final parameter set is searched automatically by the simulated annealing algorithm to have minimum χ^2.

Besides neutron and proton potentials, the following global potentials were employed in the evaluations for composite particles:

- Deuterons: Perey and Perey [15]

- Tritons: Becchetti and Greenlees [16]

- Alphas: Arthur and Young [17]

Recent work in nuclear reaction theory has emphasized the importance of calculating direct inelastic scattering cross sections to low-lying states. Such direct reaction contributions to inelastic scattering from discrete states were provided by a DWBA calculation with deformation parameters or a coupled-channel calculation with appropriate collective models.

3. Giant Dipole Resonance and Quasi-deuteron Model

There is no nuclear force and charge interaction between the photon and the nucleus, and thus the photonuclear reaction is induced by electromagnetic interaction. At low energies, below about 30 MeV, the Giant-Dipole Resonance (GDR) is the dominant excitation mechanism, where a collective bulk oscillation of the neutrons against the protons occurs. At higher energies below 140 MeV, the threshold for the pion production, where the wavelength of the photon decreases, the photoabsorption on a neutron-proton pair(quasi-deuteron: QD) which has a large dipole moment becomes important. Therefore, the photoabsorption cross section can be expressed as the sum of $\sigma_{\mathrm{GDR}}(\varepsilon_\gamma)$ and $\sigma_{\mathrm{QDM}}(\varepsilon_\gamma)$,

$$\sigma_{abs}(\varepsilon_\gamma) = \sigma_{\mathrm{GDR}}(\varepsilon_\gamma) + \sigma_{\mathrm{QDM}}(\varepsilon_\gamma). \tag{4}$$

In this work, photoabsorption cross sections in the GDR region were evaluated with GUNF code [18], in which E_1 and E_2 radiations are considered. The formulas of strength functions for E_1 and E_2 radiations used in the code are:

1. Lorentzian form with energy-dependent damping width for E_1 radiation [19]:

$$f_{E_1}(\varepsilon_\gamma) = \sum_{i=1}^{n} \frac{\sigma_i \varepsilon_\gamma \Gamma_i \Gamma_i(\varepsilon_\gamma)}{(\varepsilon_\gamma^2 - E_i^2)^2 + \varepsilon_\gamma^2 \Gamma_i^2(\varepsilon_\gamma)} \tag{5}$$

   with

$$\Gamma_i(\varepsilon_\gamma) = \Gamma_i \frac{\varepsilon_\gamma^2 + 4\pi^2 T^2}{E_i^2} \tag{6}$$

   where σ_i, E_i, and Γ_i denote the peak cross section, peak energy, and width at half-maximum of the i-th peak.

2. Lorentzian strength function for E_2 radiation:

$$f_{E_2}(\varepsilon_\gamma) = \frac{\sigma \varepsilon_\gamma^{-1} \Gamma^2}{(\varepsilon_\gamma^2 - E^2)^2 + \varepsilon_\gamma^2 \Gamma^2} \tag{7}$$

   where Γ denote the width at half-maximum of E_2 radiation.

The QDM photoabsorption cross section $\sigma_{\mathrm{QDM}}(\varepsilon_\gamma)$ is expressed in terms of the quasi-deuteron model which uses a Levinger-type theory to relate the nuclear photoabsorption cross section to the experimental deuteron photodisintegration cross section $\sigma_d(\varepsilon_\gamma)$,

$$\sigma_{QDM}(\varepsilon_\gamma) = L \frac{NZ}{A} \sigma_d(\varepsilon_\gamma) f(\varepsilon_\gamma) \tag{8}$$

where the Levinger parameter was derived to be $L = 6.5$, and $f(\varepsilon_\gamma)$ is the Pauli-blocking function, which reduces the free deuteron cross section $\sigma_d(\varepsilon_\gamma)$ to account for Pauli-blocking of the excited neutron and proton by the nuclear medium. NZ is the total number of neutron-proton pairs inside the nucleus, and the free deuteron cross section is as follows:

$$\sigma_d(\varepsilon_\gamma) = 61.2 \frac{(\varepsilon_\gamma - 2.224)^{\frac{3}{2}}}{\varepsilon_\gamma} \mathrm{mb}. \tag{9}$$

4. Equilibrium and Preequilibrium Emission

After the above steps have been completed, all model parameters are available for the decay processes including n, p, d, t and α particle emission. The latest version of the GNASH code [20] has been used to calculate nuclear reaction cross sections using the Hauser-Feshbach theory for equilibrium decay and the exciton model for preequilibrium decay. The Hauser-Feshbach theory with full angular momentum and parity conservation calculated the equilibrium emission [21]. The exciton model was used to describe the processes of preequilibrium emission, and damping to equilibrium, during the evolution of the reaction. The file of discrete level information and ground-state masses, spin and parities were provided [22]. The mass values were based upon 1995 Audi compilation [23], and supplemented in the case of unmeasured masses with values from the Moller and Nix calculations [24].

The Ignatyuk [25] nuclear level densities are used, which include the washing-out of shell effects with increasing excitation energy, and are matched continuously onto low-lying experimental discrete levels. The Ignatyuk model for describing the statistical level density properties of excited nuclei is particularly appropriate for the relatively high energies studied in this work.

5. Compilation of Cross Sections

Evaluated cross sections are then compiled utilizing MF3-MT5 and MF6-MT5 combinations in the ENDF6 format which is suitable for a complete representation of the high energy reaction data. The total nonelastic cross section is tabulated in MF3-MT5, whereas the inclusive production cross sections (emission multiplicities) and emission spectra for neutron, proton, deuteron, triton, alpha particles, and all residual nuclides are tabulated by use of MF6-MT5. Descriptions of ENDF6 formats for each incident particle are summarized in Table 1, 2, and 3.

Table 1: ENDF format of the Neutron Library

MF=3	MT= 1	total cross section
	MT= 2	elastic scattering cross section
	MT= 3	nonelastic cross section
	MT= 5	sum of binary (n,n') and (n,x) reactions
MF=4	MT= 2	elastic angular distributions
MF=6	MT= 5	production cross sections and energy-angle distributions for Emission neutrons, protons, deuterons, and alphas; and angle-integrated spectra for gamma rays and residual nuclei that are stable against particle emission

Table 2: ENDF format of the Proton Library

MF=3	MT= 2	integral of nuclear plus interference components of the elastic scattering cross section
	MT= 5	sum of binary (p,n') and (p,x) reactions
MF=6	MT= 2	elastic angular distributions given as ratios of the differential nuclear-plus-interference to the integrated value.
	MT= 5	production cross sections and energy-angle distributions for emission neutrons, protons, deuterons, and alphas; and angle-integrated spectra for gamma rays and residual nuclei that are stable against particle emission

Table 3: ENDF format of the Photon Library

MF=3	MT= 5	photoabsorption cross section
MF=6	MT= 5	production cross sections and energy-angle distributions for emission neutrons, protons, deuterons, and alphas; and angle-integrated spectra for gamma rays and residual nuclei that are stable against particle emission

III. Results and Comparisons with Measurements

1. Neutron- and Proton-Nucleus Reaction Cross Sections

Total, Reaction Cross Sections Elastic Angular Distributions: The total (for neutron) and reaction (for proton) cross sections, and elastic angular distributions from the optimized optical model parameters for some selected isotopes are compared in Fig. 2 with the reference measurements as well as other data not adopted as references. The optimized optical model parameters give overall agreement with most of the experimental data over the entire energy range for both incident neutrons and protons. It is also noted that for incident energies below around 10 MeV, the optical model cross sections describes the smoothed average of the resonance structures well.

Direct Inelastic Scattering Cross Sections: The soft rotator model [26] was applied for the direct inelastic scattering to the low-lying collective states for some structural materials such as Si-28, Fe-56, Cr-52, and Ni-58. Figure 3 demonstrates the comparison of experimental and predicted collective level schemes for ^{58}Ni. Figure 4 compares experimental and calculated angular distributions for neutrons scattered to the 2^+ (1.454 MeV) level with the soft rotator models based on the predicted collective level schemes. It was found that the model is modestly successful in describing the collective low-lying level structure of some structural material which exhibits neither the typical rotational nor the vibrational spectra.

Production and Emission Cross Sections: The left hand side of figure 5 compares the evaluated ^{23}Na isotope production cross sections of incident neutron on ^{27}Al against Los Alamos data [27] together with evaluations from LANL and JENDL. The production cross sections consists of emission reactions of (n,na), (n,dt), (n,npt), (n,n2d), (n,2npd) and (n,3n2p) to give the residual ^{23}Na isotope. Our evaluated cross sections and other two evaluated ones give good agreements with the measured data in energies from the threshold up to 45 MeV. Around the neutron energy of 22 MeV having peak cross sections, our evaluations are slightly closer to the measurements than the other two. Above the neutron energy of 45 MeV, all evaluated cross sections have similar values to have lower cross sections than the measurements. Right hand side of Figure 5 simply shows emission spectra at 30 degree of 90 MeV (p,xn) reaction of ^{27}Al compared with measurements [28] and LANL evaluation. It reproduced a general shape of emission spectra showing both equilibrium and preequilibrium decays.

Proton-induced activation cross sections: Figure 6 shows selected comparisons of the proton-induced cross sections for which the evaluations are focused on the medical and activation analyses applications. In the model calculations, the level density parameters and the composite nucleus state density constants of the preequilibrium model are slightly adjusted to better reproduce the measurements for some reaction channels.

2. Photonuclear Reaction Cross Sections

As an example of evaluated photonuclear cross sections in the KAERI library, ^{34}S and ^{120}Sn cases are briefly described here.

^{34}S : The photoabsorption cross section was evaluated based on the experimental data of Assafiri [29], up to 35 MeV. Above this energy, the absorption cross section was calculated from the

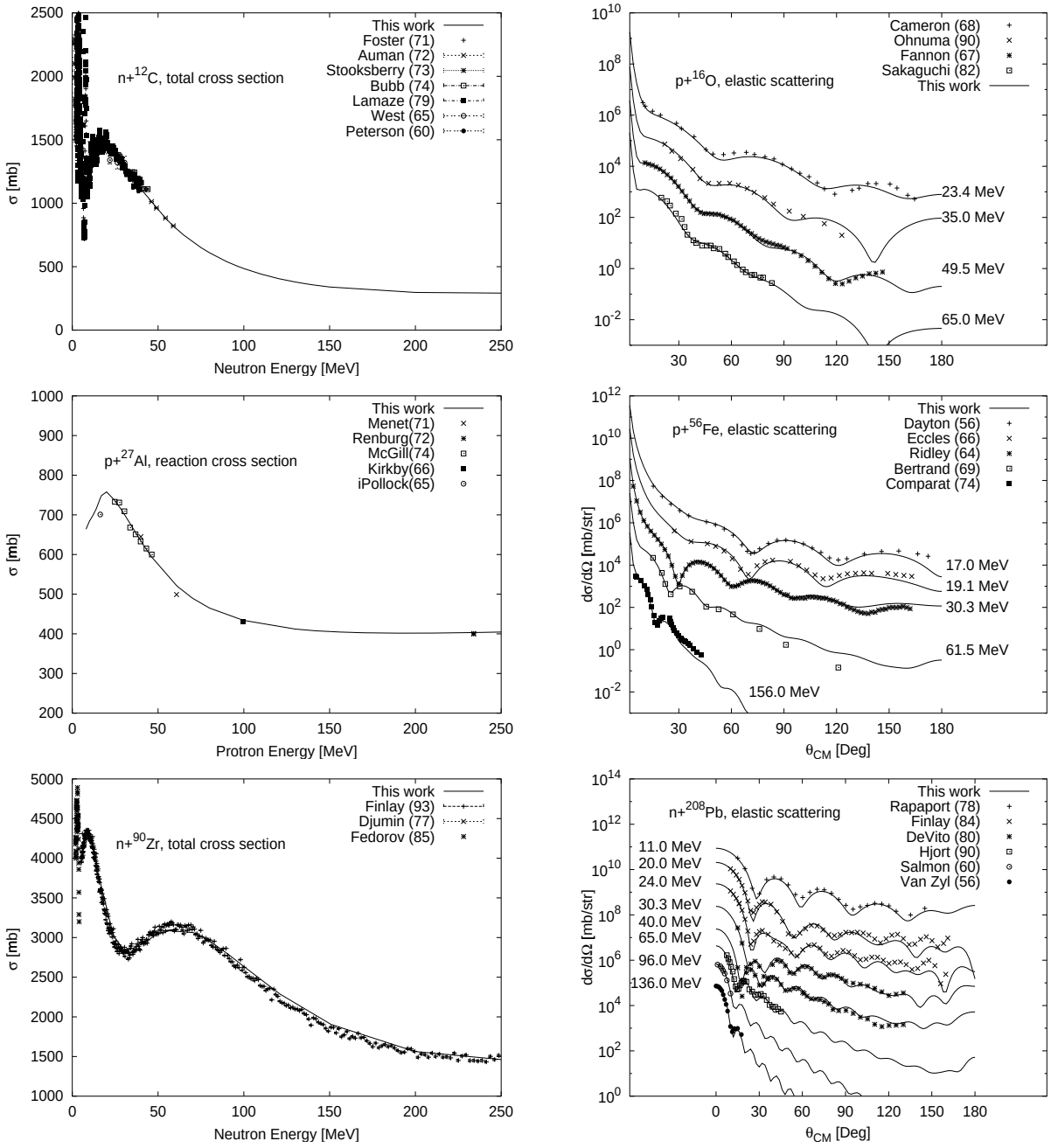

Figure 2: Total, reaction cross section and elastic angular distribution for neutron- and proton-induced reactions calculated by the optical model analyses

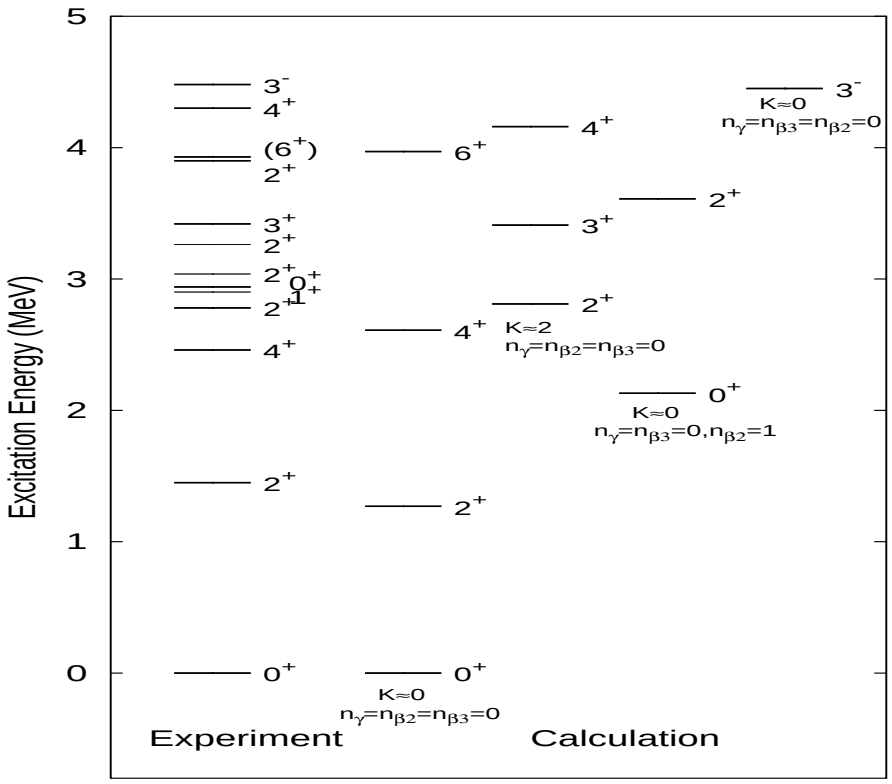

Figure 3: Comparison of the experimental and calculated level schemes for ^{58}Ni. Thick lines show experimental levels describes by the soft-rotator model

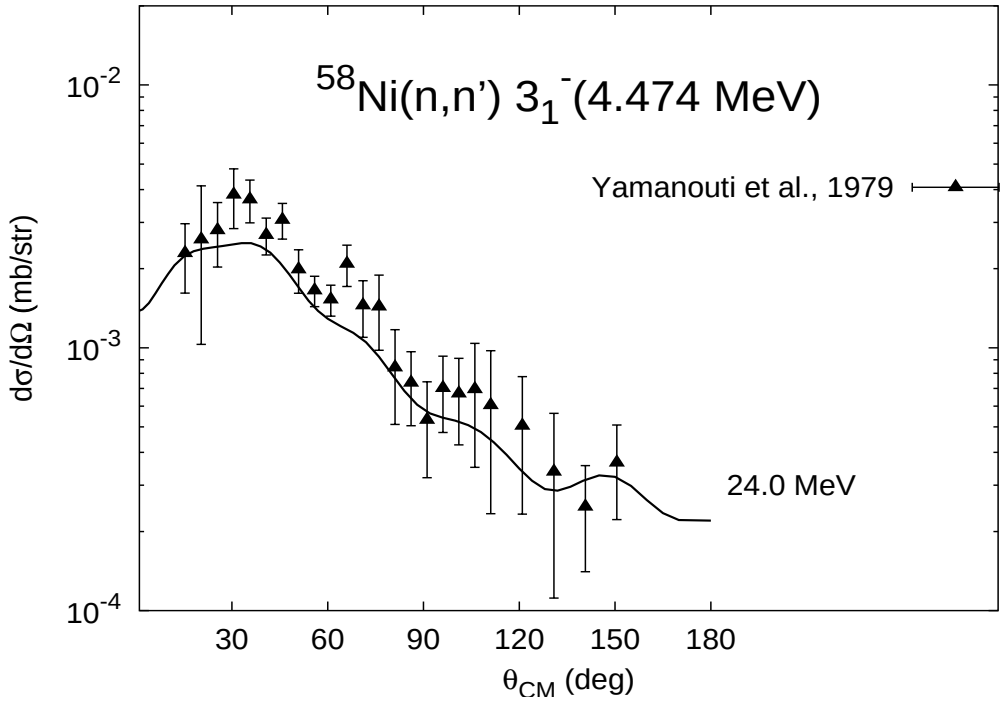

Figure 4: Comparison of experimental and calculated angular distribution for neutrons scattered to the 3^- (4.475 MeV) level of the ^{58}Ni. Solid lines : Present calculation.

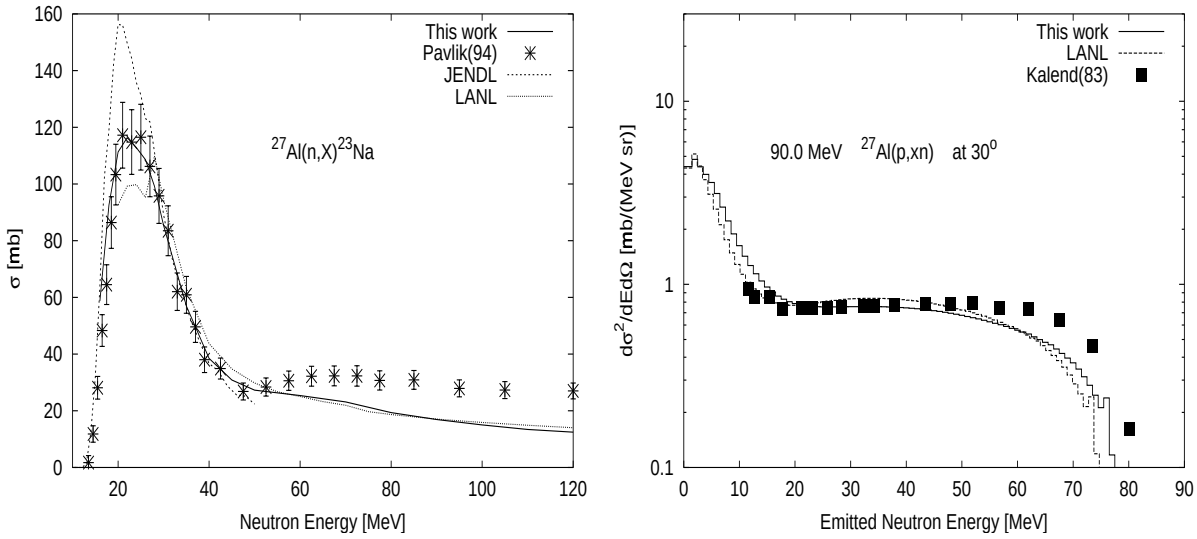

Figure 5: Left: Evaluated ^{23}Na production cross sections of neutron for ^{27}Al . including reactions (n,na), (n,dt), (n,npt), (n,n2d), (n,2npd), (n,3n2p), (n,n2d) (n,2npd) (n,3n2p). Right: Neutron emission spectra at 30 degree of 90 MeV (p,xn) reaction on ^{27}Al

QD model. In Fig. 7, the calculated results of the emission channels by the GNASH code are in good agreement with the experimental data [29, 30] for the (γ, sn) and (γ, p) reaction cross sections, but there are some gaps between calculations and measurements for (γ, 2n) reaction cross sections above around 25 MeV of photon energies.

^{120}Sn : There are no measurements of the photoabsorption cross section in the GDR energy region. But Lepretre [31] and Fultz [32] measured the (γ, 1nx), (γ, 2nx), (γ, sn) and (γ, xn) reaction cross sections. Lepretre [33] also measured the photoabsorption cross section for ^{nat}Sn from 25 MeV to 135 MeV. We relied on the GUNF and GNASH codes to infer the photoabsorption cross section in the GDR regime, using Lepretre's two measurements [31, 33], in order to model all the photonuclear cross sections consistently, as shown Fig. 7. The photoabsorption cross section above the GDR, up to 140 MeV, was obtained from QD model calculations using the theory of Chadwick. The neutron emission as well as production were theoretically calculated and compared with the measurements also in Fig. 7.

IV. Summary

Neutron Library: The KAERI neutron library currently has 10 isotopes such as C-12, N-14, O-16, Al-27, Si-28, Ca-40, Fe-56, Ni-58, Zr-90, Sn-120, and Pb-208 for energies from 20 up to 400 MeV. The library provides nuclear data needed for transport and shielding applications. The evaluation is based on nuclear model calculations that have been benchmarked to experimental data. Energy dependent optical model parameters of neutron and proton were searched to obtain particle transmission coefficients, as well as for describing measured total, reaction and elastic scattering cross sections. Compound reaction calculations with preequilibrium corrections were performed using the GNASH code. Direct reaction contributions to inelastic scattering were provided by DWBA or coupled channel calculations.

Proton Library: The proton nuclear data were evaluated in a consistent manner with the neutron case, using the same nuclear model parameters. In addition to the same isotopes in the neutron library, proton library has 70 extra isotopes of 24 elements ranging from nitrogen to lead up to 150 MeV for which the evaluations are focused on the medical and activation analyses

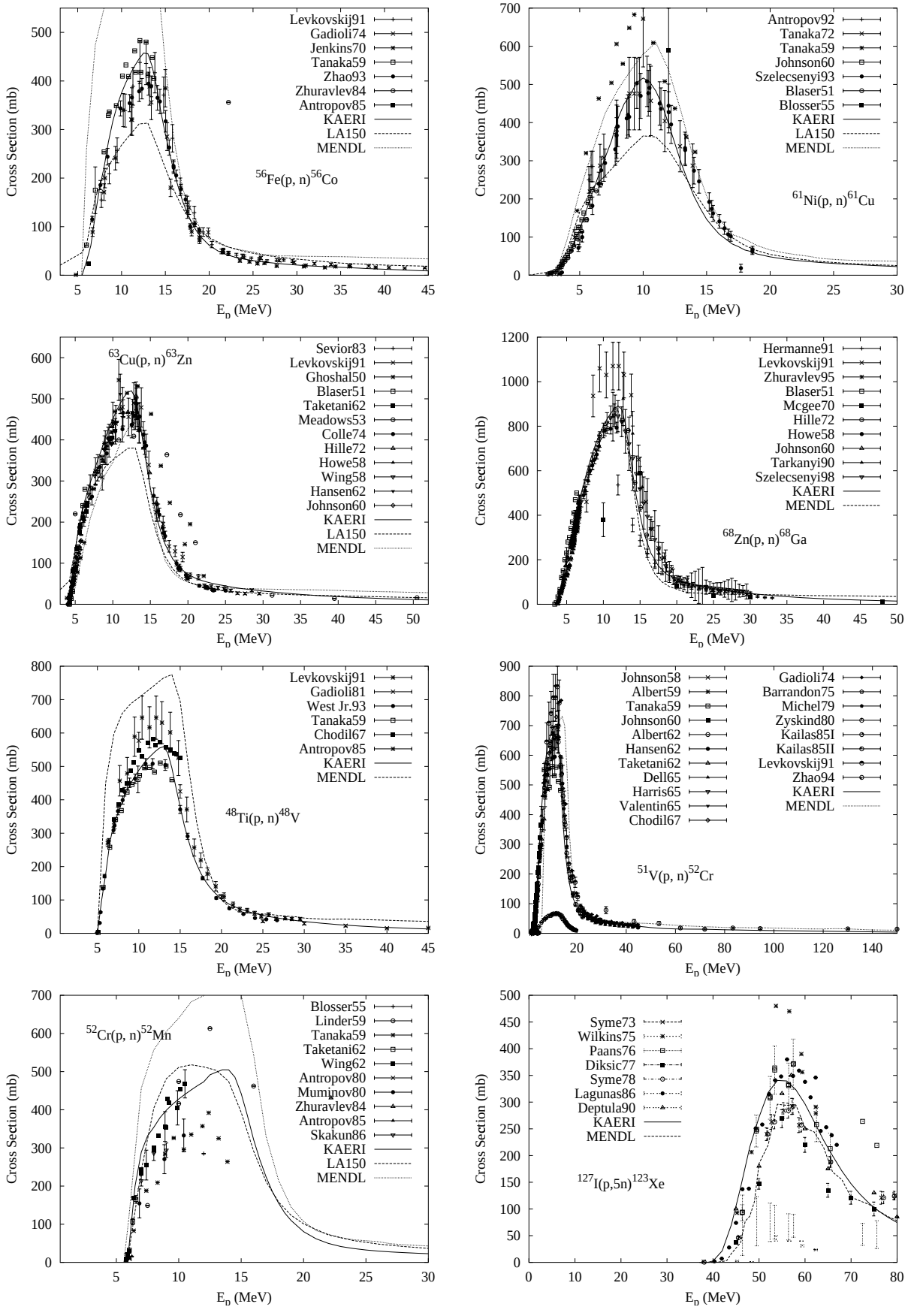

Figure 6: Selected comparisons of proton-induced activation cross sections in the KAERI proton library with measurements, LA150, and MENDL

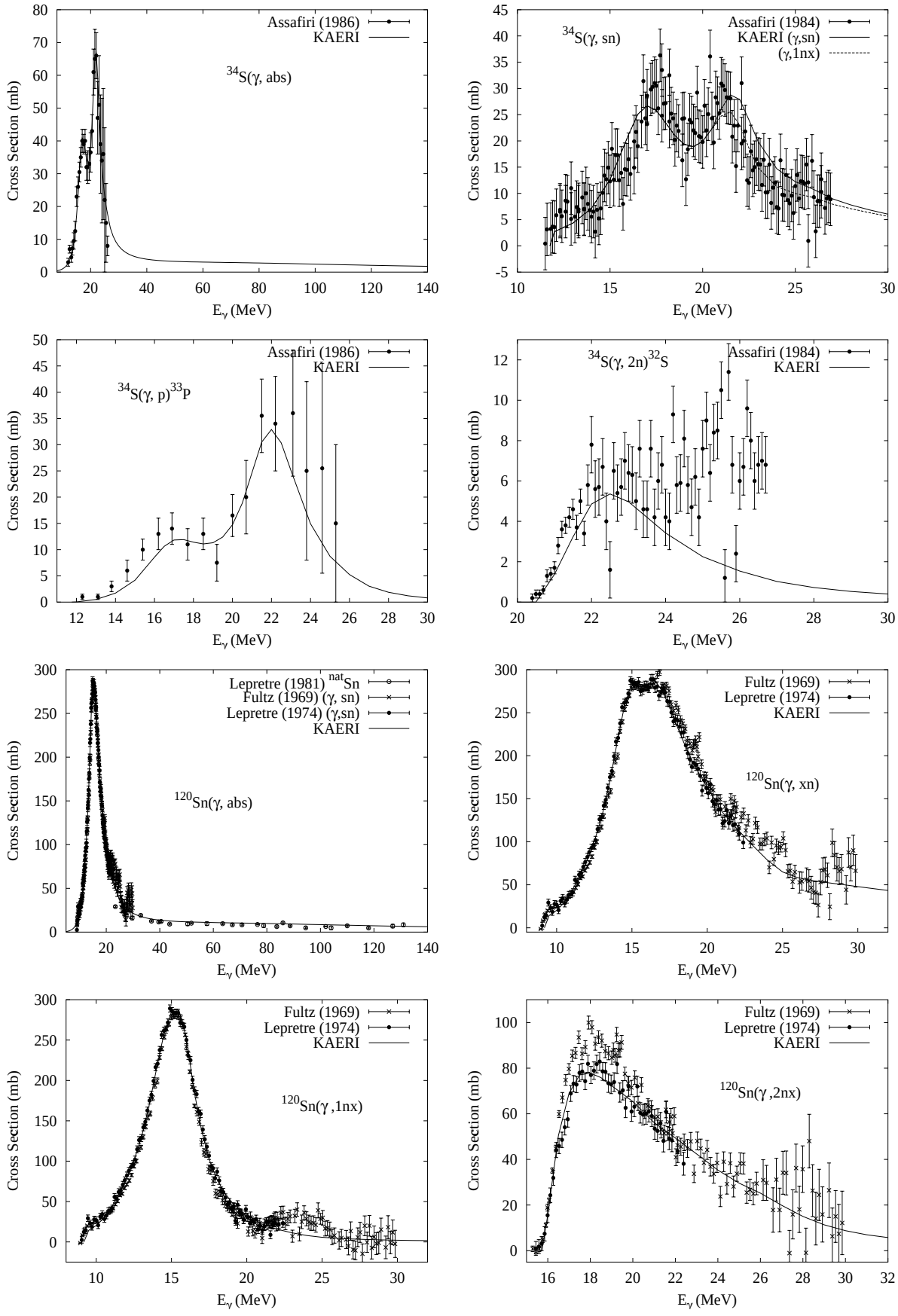

Figure 7: Photonuclear cross sections for ^{34}S and ^{120}Sn included in the KAERI Photonuclear Data Library

applications. The list of evaluated radioisotopes was obtained from IAEA-TECDOC-924 for thin layer activations and from INDC(NDS)-388 for medical radioisotope production.
Photon Library: KAERI photonuclear data library has been built along with international collaboration by participating in the IAEA's Coordinated Research Project (CRP) during 1997 - 2000. Currently 143 isotopes of 39 elements are included in the KAERI photonuclear data library. Available experimental data were collected and their discrepancies were analyzed to select or to reconstruct the representative data set. The photoabsorption cross sections were then evaluated by applying the Giant Dipole Resonance (GDR) model for energies below about 30 MeV, and the quasi-deuteron model for energies below 140 MeV. The GDR parameters are adjusted automatically by fitting the experimental data of photoabsorption or photoneutron cross sections. The resulting representative photoabsorption data were given as input for theoretical calculations for the emission process of neutron, proton, deuteron, triton, He-3, alpha particles and gamma rays using GNASH code.

Acknowledgements

This work was performed under the auspices of Korea Ministry of Science and Technology as one of the long-term nuclear R&D programs. Two of the authors (Y.H and E.Sh.S.) are grateful to the Korea Ministry of Science and Technology, the Korea Science and Engineering Foundation, and Korea Institute of Science and Technology Evaluation Planning for giving them opportunities to carry out parts of this work.

References

[1] Y. O. Lee, T. Fukahori, J. Chang, and C. S., "Evaluation of Neutron- and Proton-induced Cross Section of Al-27 up to 2 GeV," in *Proc. of the 1998 Symposium on Nuclear Data, Nov. 19-20, 1998, JAERI, Tokai, Japan*, no. JAERI-Conf 99-002, p. 246, 1999.

[2] Y. O. Lee, T. Fukahori, J. Chang, and C. S., "Evaluation of Neutron- and Proton-induced Cross Section of Al-27 up to 2 GeV," *J. of Nucl. Sci. and Tech.*, vol. 36, no. 12, p. 1125, 1999.

[3] Y. O. Lee, T. Fukahori, J. Chang, and C. S., "Optical model potential search for neutron- and proton induced reactions of ^{12}C, ^{16}O, ^{27}Al, ^{56}Fe, ^{90}Zr and ^{208}Pb up to 250 MeV," in *Proc. of PHYSOR 2000: ANS International Topical Meeting on Advances in Reactor Physics and Mathmatics and Computation into the Next Millenium*, Pittsburgh, Pennsylvania, U.S.A, May 7-12, 2000, 2000.

[4] Y. O. Lee, J. Chang, and M. Kim, "Parameterization and Optical Model Analyses of Proton-Nucleus Cross Sections for Space Shielding," *IEEE Transactions on Nuclear Science*, vol. 47, no. 6, p. 2435, 2000.

[5] D. Kim, Y. O. Lee, and J. Chang, "Calculation of Proton-Induced Reactions on Ti, Fe, Cu and Mo up to 60 MeV for TLA Applications," *Journal of Korean Nuclear Society*, vol. 31, p. 595, 1999.

[6] D. Kim, Y. Han, and J. Chang, "Calculation of Proton-Induced Reactions on Tellurium Isotopes below 60 MeV for Medical Radioisotope Production," *Journal of Korean Nuclear Society*, vol. 32, p. 361, 2000.

[7] D. Kim, "Evaluation of Proton-Induced Nuclear Reaction Data for Sn, Sb, Te, I, Xe, Cs, Fe, Ni, Cu, Zn, Ti, V, Cr, Nb, and Mo Isotopes up to 150 MeV at KAERI," Tech. Rep. NDL-21/00, NDL-03/01, NDL06-01, KAERI, 2000-2001.

[8] Y. O. Lee, T. Fukahori, and J. Chang, "Evaluation of Photonuclear Reaction Data on Tantalum-181 up to 140 MeV," *J. of Nucl. Sci. and Tech.*, vol. 35, p. 685, 1998.

[9] Y. O. Lee, Y. Han, and J. Chang, "Evaluation of Photonuclear Data of Mo, Zn, S and Cl for Medical and Accelerator Applications," in *Proc. of 9th International Conference on Radiation Shielding*, Tsukuba, Japan, Oct. 17-22, 1999.

[10] Y. O. Lee, Y. Han, J. Lee, and J. Chang, "Evaluated Photonuclear Data Library in KAERI," in *Proc. of the Korean Nuclear Society Autumn Meeting*, Seoul, Korea, Oct. 29-30, 1999.

[11] OECD/NEA, Data Bank, WWW address: http://www.nea.fr.

[12] A. J. Koning, J. P. Delaroche, and O. Bersillon, "Neutron and proton data files up to 150 MeV for 54Fe, 56Fe, 58Ni and 60Ni," Tech. Rep. ECN-RX-97-047, Netherlands Energy Research Foundation ECN, Petten, The Netherlands, 1997.

[13] Y. O. Lee, "ECISPLOT: An Interactive Optical Model Parameter Searcher with Simulated Annealing Algorithm," Tech. Rep. NDL-9/99, KAERI, 1999.

[14] J. Raynal, "Notes on ECIS94," Tech. Rep. CEA-N-2772, pp. 1–145, Commisariat á l'Energie Atomique (CEA), Saclay, France, 1994.

[15] C. M. Perey and F. G. Perey, "Compilation of Phenomenological Optical Model Parameters," *Atomic Data and Nucl. Data Tables*, vol. 17, pp. 1–101, 1976.

[16] F. D. Becchetti and G. W. Greenlees in *Proc. of the Conference on Polarization Phenomena in Nuclear Reactions* (H. Barschall and W. Haeberli, eds.), (University of Wisconsin), p. 682, University of Wisconsin Press, 223, 1971.

[17] P. G. Young, "Ch4: Optical Model Parameters," Tech. Rep. IAEA TECDOC-1034, International Atomic Energy Agency, Vienna, Austria, 1998.

[18] J. Zhang, "Illustration of Photonuclear Data Calc. with GUNF Code," *Commu. of Nucl. Data Prog.*, vol. 19, p. 33, 1998.

[19] J. Kopecky and M. Uhl, "Test of Gamma-Ray Strength Functions in Nuclear-Reaction Model-Calculations," *Phys. Rev. C*, vol. 41, pp. 1941–1955, 1990.

[20] P. G. Young, E. D. Arthur, and M. B. Chadwick, "Comprehensive nuclear model calculations: Theory and use of the GNASH code," in *Proc. of the IAEA Workshop on Nuclear Reaction Data and Nuclear Reactors - Physics, Design, and Safety* (A. Gandini and G. Reffo, eds.), (Singapore), pp. 227–404, Trieste, Italy, April 15 - May 17, 1996, World Scientific Publishing, Ltd., in press.

[21] M. B. Chadwick, P. G. Young, and S. Chiba, "Photonuclear angular distribution systematics in the quasideuteron regime," *Journal of Nuclear Science and Technology*, vol. 32, p. 1154, 1995.

[22] R. B. Firestone and V. S. Shirley, *Table of Isotopes, 8th edition*. New York, NY: John Wiley and Sons, 1996.

[23] G. Audi and A. Wapstra *Nucl. Phys.*, vol. A595, p. 409, 1995.

[24] P. Moeller, J. Nix, W. Myers, and W. Swiatecki *Atomic Data and Nuclear Data Tables*, vol. 59, p. 185, 1995.

[25] A. V. Ignatyuk, G. N. Smirenkin, and A. Tishin, "Phenomenological Description of the Energy Dependence of the Level Density Parameter," *Sov. J. Nucl. Phys.*, vol. 21, pp. 255–257, 1975.

[26] E. Sukhovitskii, Y.-O. Lee, J. Chang, S. Chiba, and O. Iwamoto, "Nucleon interaction with ^{58}Ni up to 150 MeV studied in the coupled-channels approach based on the soft-rotator nuclear structure model," *Phys. Rev. C*, vol. 62, p. 044605, 2000.

[27] H. Hitzenberger, A. Pavlik, H. Vonach, M. B. Chadwick, R. C. Haight, R. O. Nelson, and P. G. Young, "Study of ^{27}Al(n,xγ) reactions up to E_n = 400 MeV," in *Proc. of the International Conference on Nuclear Data for Science and Technology* (J. K. Dickens, ed.), (La Grange Park, IL), pp. 367–370, Gatlinburg, TN, 1994, American Nuclear Society, 1994.

[28] A. M. Kalend, B. D. Anderson, A. R. Baldwin, R. Madey, J. W. Watson, C. C. Chang, H. D. Holmgren, R. W. Koontz, J. R. Wu, and H. Machner, "Energy and Angular Distributions of Neutrons from 90 MeV Proton and 140 MeV Alpha-Particle Bombardment of Nuclei," *Phys. Rev. C*, vol. 28, pp. 105–118, 1983.

[29] Y. Assafiri, G. Egan, and M. Thompson, "Photoproton Cross Section of ^{34}S," *Nucl. Phys.*, vol. A460, p. 455, 1986. EXFOR M0510.

[30] Y. Assafiri, G. Egan, and M. Thompson, "Photoneutron Cross Section of ^{34}S," *Nucl. Phys.*, vol. A413, p. 416, 1984. EXFOR M0506.

[31] A. Lepretre, H. Beil, R. Bergere, P. Carlos, A. Deminiac, and A. Veyssiere, "A study of the giant dipole resonance of vibrational nuclei in the 103-a-133 mass region," *Nucl. Phys. A*, vol. 219, p. 39, 1974. EXFOR L0035.

[32] S. Fultz, B. Berman, J. Caldwell, R. Bramblett, and M. Kelly, "Photoneutron cross sections for Sn-116, Sn-117, Sn-118, Sn-119, Sn-120, Sn-124, and indium," *Phys. Rev.*, vol. 186, p. 1255, 1969. EXFOR L0017.

[33] A. Lepretre, H. Beil, R. Bergere, P. Carlos, J. Fagot, A. DeMiniac, and Veyssiere, "The measurements of the total photonuclear cross sections from 30 MeV to 140 MeV for Sn, Ce, Ta, Pb and U nuclei," *Nucl. Phys. A*, vol. 367, p. 237, 1981.